

Supplementary Materials for  
**Clonal dominance defines metastatic dissemination in pancreatic cancer**

I-Lin Ho *et al.*

Corresponding author: Andrea Viale, [aviale@mdanderson.org](mailto:aviale@mdanderson.org); I-Lin Ho, [ihho@mdanderson.org](mailto:ihho@mdanderson.org);  
Chieh-Yuan Li, [alexcyli2015@gmail.com](mailto:alexcyli2015@gmail.com)

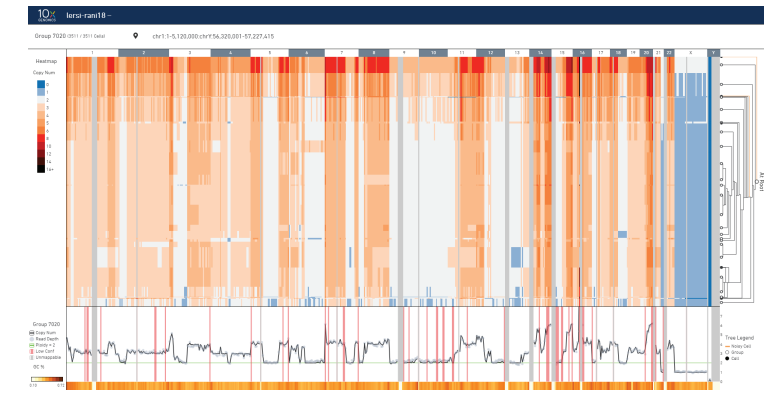
*Sci. Adv.* **10**, eadd9342  
DOI: 10.1126/sciadv.add9342

**This PDF file includes:**

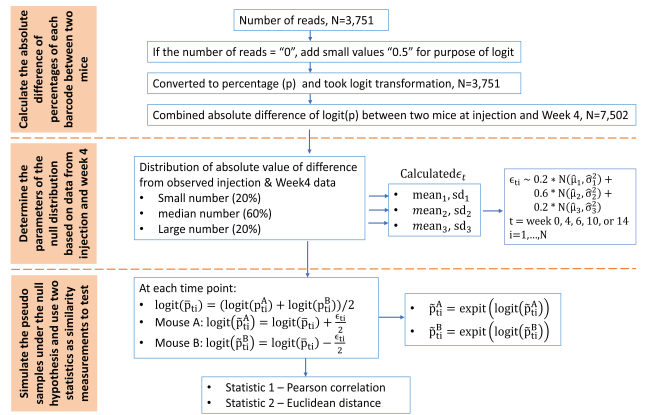
Figs. S1 to S6

**Fig. S1**

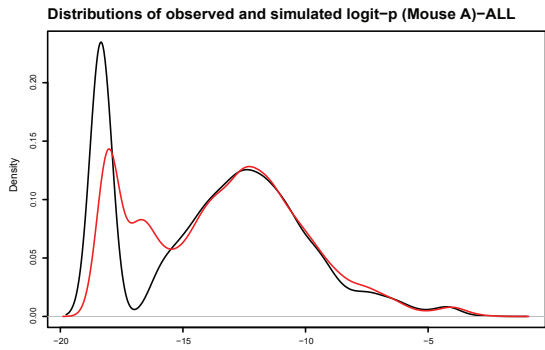
**A**



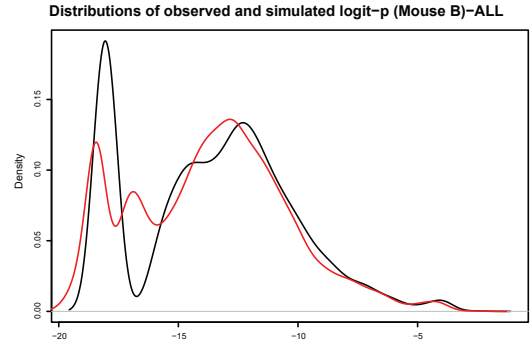
**B**



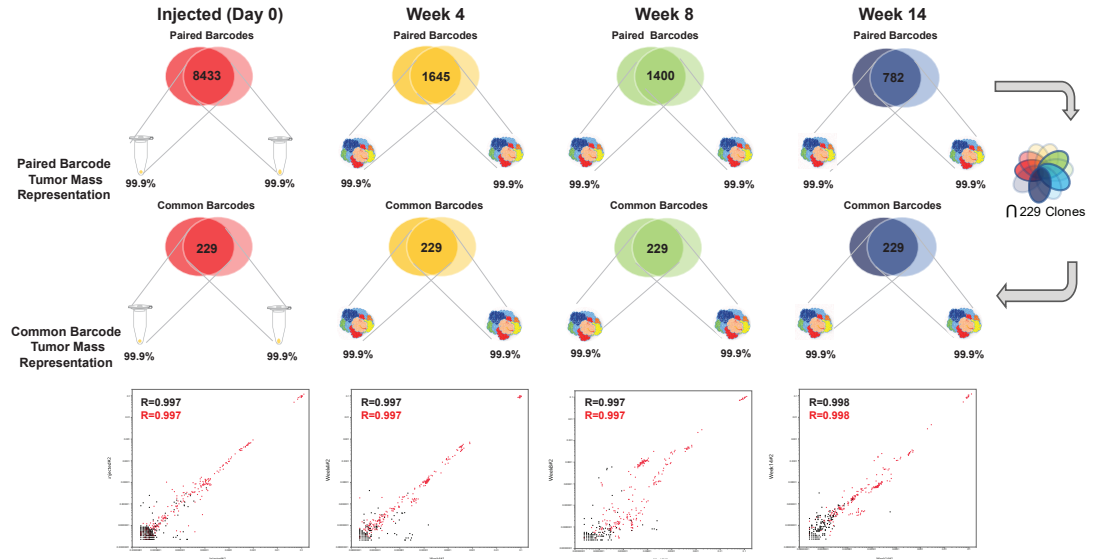
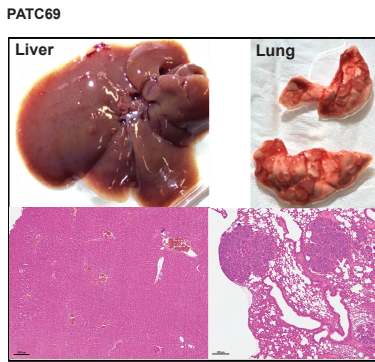
**C**



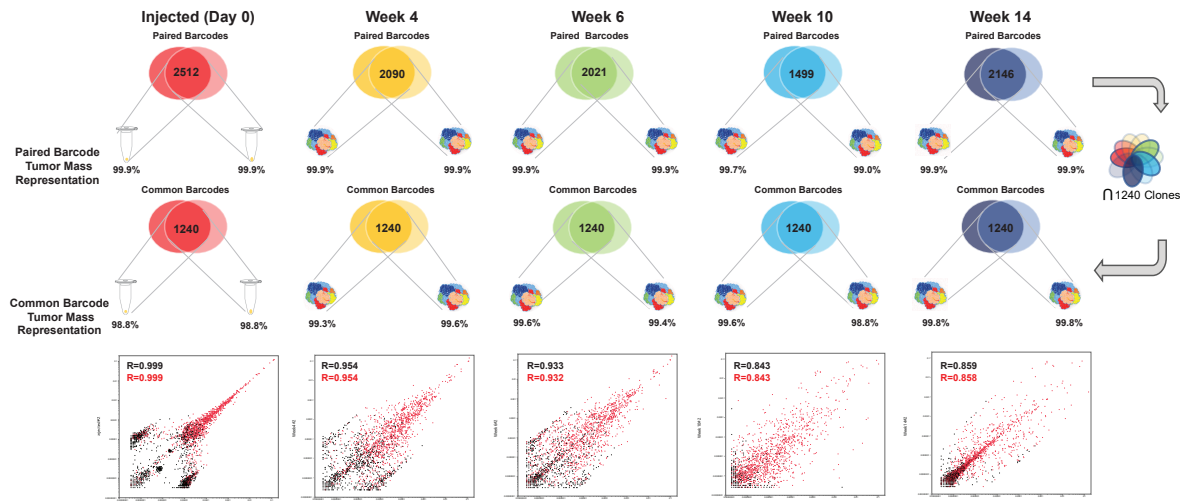
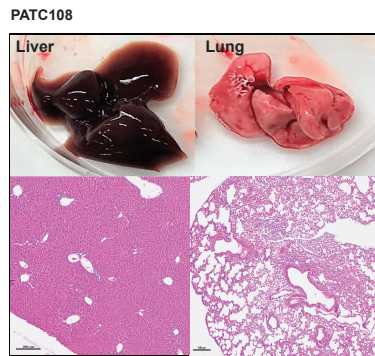
**D**



**E**



**F**

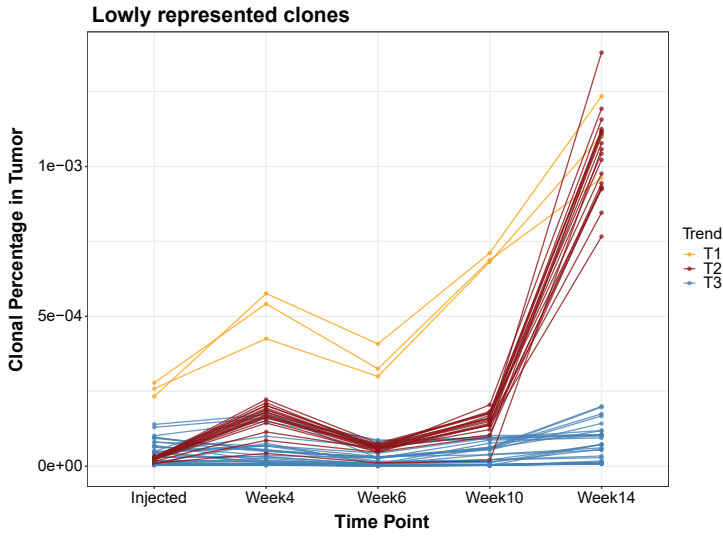


**Supplementary Figure 1. oCRTs capture unperturbed clonal dynamics in different PDX-derived cells.**

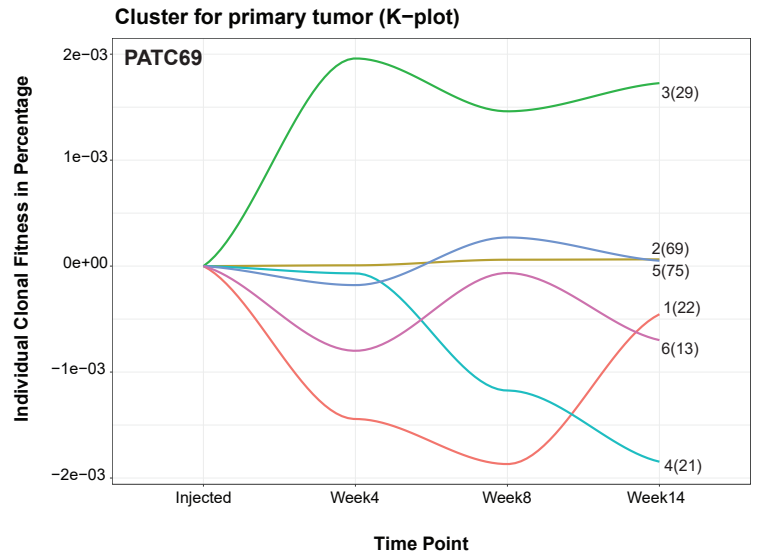
**a**, Single-cell CNV analysis of PATC124 cells through 10x Genomics platform (n=3,511 cells). Columns indicate chromosome number. Red, copy number gain; blue, copy number loss; bottom, average CNV profile of all cells; right, clustering of detected subclones. **b**, Flow of barcode data processing, simulation and resampling bootstrap test for PATC124 oCRTs. **c,d**, Observed distribution of logit-transformed percentages of two PATC124 oCRT samples (mouse A (**c**) and B (**d**)) for all timepoints were combined (black line). At each timepoint, assuming one randomly picked mouse as A and another one as B. The simulated distributions for all timepoints were combined and shown in red. Assuming  $\text{logit}(\bar{p}_{ti}) = (\text{logit}(p_{ti}^A) + \text{logit}(p_{ti}^B))/2$ ;  $\text{logit}(\tilde{p}_{ti}^A) = \text{logit}(\bar{p}_{ti}) + \frac{\epsilon_{ti}}{2}$ ,  $\text{logit}(\tilde{p}_{ti}^B) = \text{logit}(\bar{p}_{ti}) - \frac{\epsilon_{ti}}{2}$  and  $\epsilon_{ti} \sim 0.2 \times N(\hat{\mu}_1, \hat{\sigma}_1^2) + 0.6 \times N(\hat{\mu}_2, \hat{\sigma}_2^2) + 0.2 \times N(\hat{\mu}_3, \hat{\sigma}_3^2)$ , timepoint  $t = \text{day } 0 \text{ or } 4, 6, 10 \text{ or } 14 \text{ weeks}$ ; barcode  $i = 1, \dots, N$ ; **e**, Left: metastatic organotropism of PATC69 transplanted mice. After three months, livers and lungs were collected for gross anatomical analysis (upper quadrants) and histological analysis (lower quadrants) (Scale bar = 200  $\mu\text{m}$ ). Right: clonal correlation among PATC69 orthotopic clonal replica tumors (oCRTs) at different time points. Top, paired barcoded lineages shared by primary tumors at each time point and their relative representation (%) of tumor mass; middle, set of 229 barcodes common to all tumors and their relative representation (%) of tumor mass; bottom, scatter plots displaying representation of individual lineages derived from  $n = 2$  tumors collected at each time point (red, set of common clones). **f**, Left: metastatic organotropism of PATC108 transplanted mice. After three months, livers and lungs were collected for gross anatomical analysis (upper quadrants) and histological analysis (lower quadrants) (Scale bar = 200  $\mu\text{m}$ ). Right: clonal correlation among PATC108 oCRTs at different time points. Top, paired barcoded lineages shared by primary tumors at each time point and their relative representation (%) of tumor mass; middle, set of 1240 barcodes common to all tumors and their relative representation (%) of tumor mass; bottom, scatter plots displaying representation of individual lineages derived from  $n = 2$  tumors collected at each time point (red, set of common clones).

**Fig. S2**

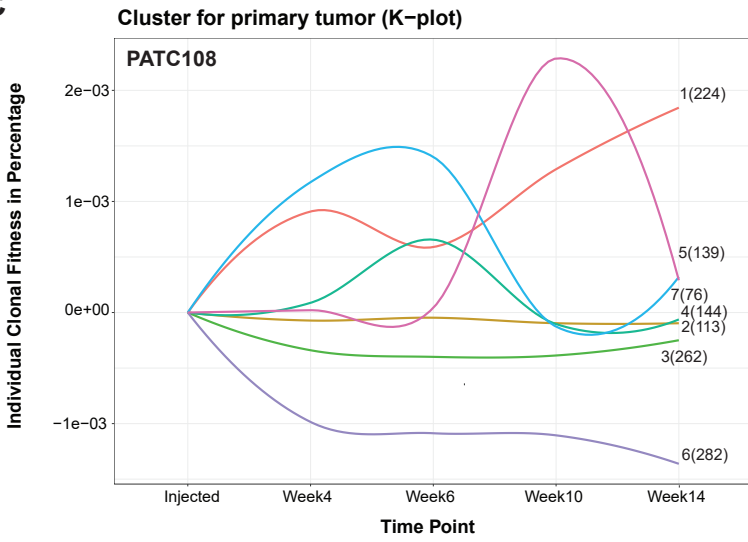
**A**



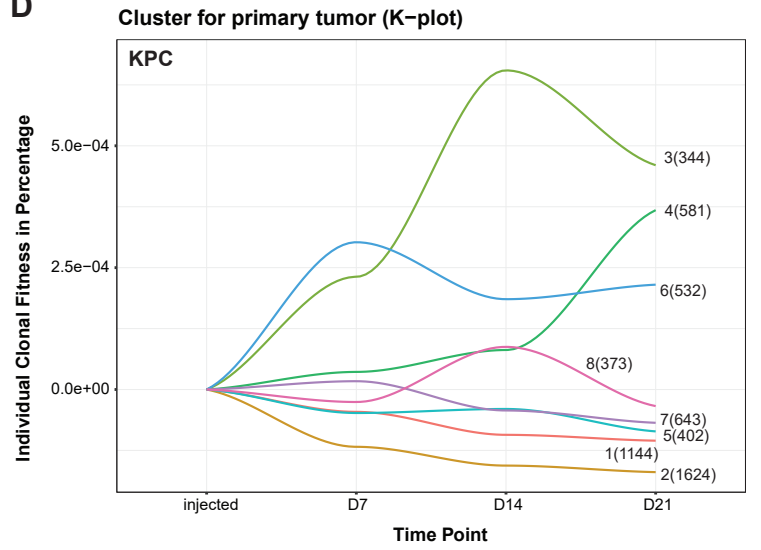
**B**



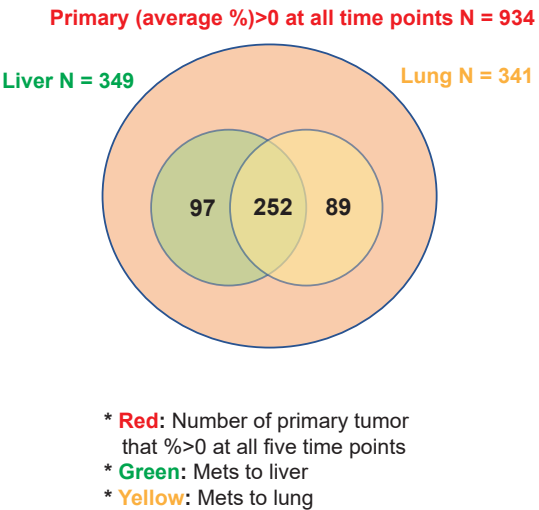
**C**



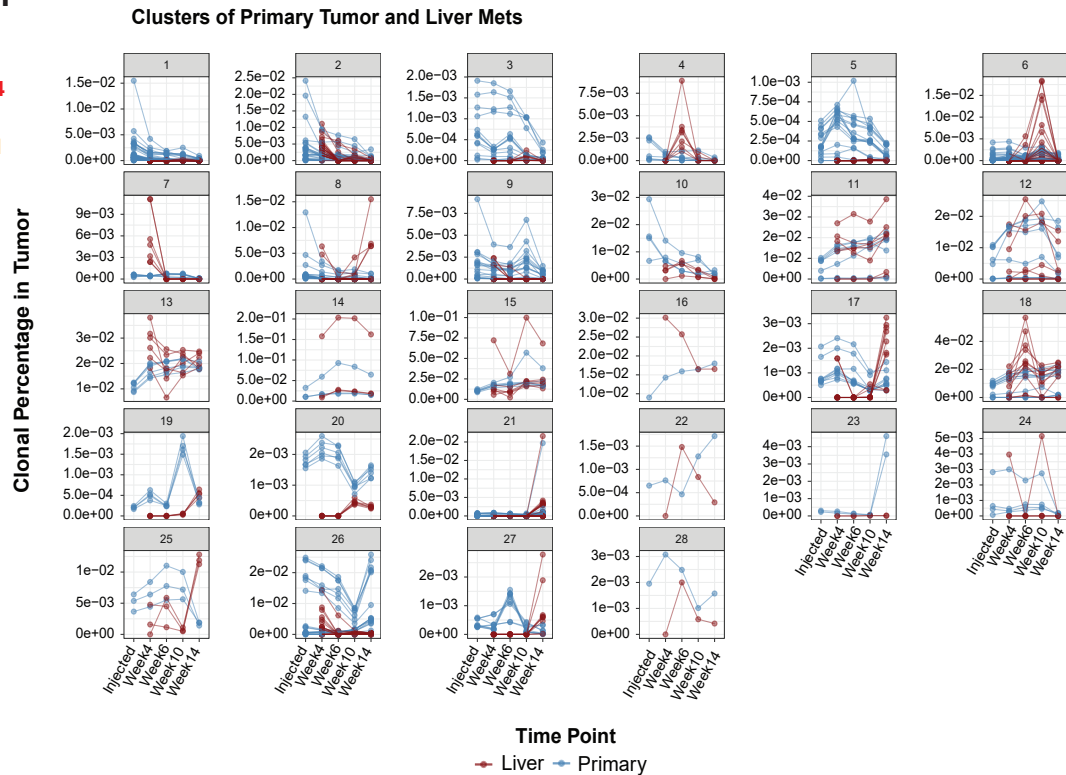
**D**



**E**



**F**



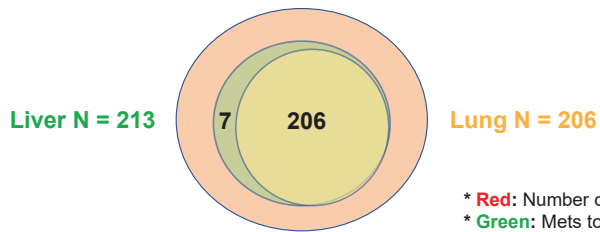
**Supplementary Figure 2. Different pancreatic cancer models show ACD during tumor expansion**

**a**, Clonal dynamics of lowly represented PATC124 clones. Each line represents growth dynamics of an individual barcode. **b-d**, Barcode analysis of  $n = 2$  PATC69 (**b**), PATC108 (**c**) and KPC (**d**) tumors per timepoint was weighted smoothed and normalized to injected samples. Barcodes were grouped into discrete dynamic growth patterns (clusters) and plotted as percent of total tumor over time (colored lines). On the right of each line, the numbers outside brackets indicate the cluster name, and numbers within brackets indicate the number of barcodes within the cluster. **e**, Venn diagram of the number of clones detected in the primary tumor, liver, and lungs of PATC124 at least at one time point. **f**, Dynamic growth of PATC124 subclones in the primary tumor (blue) overlaid with their behavior in the liver (red).

**Fig. S3**

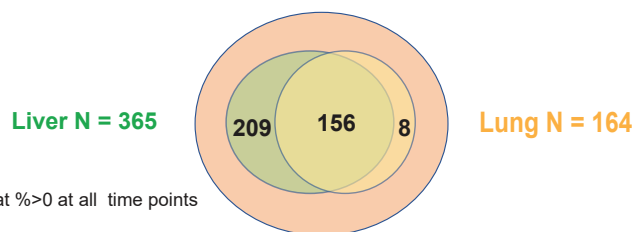
**A**

Primary (average %)>0 at all time points N = 229



**B**

Primary (average %)>0 at all time points N = 1240

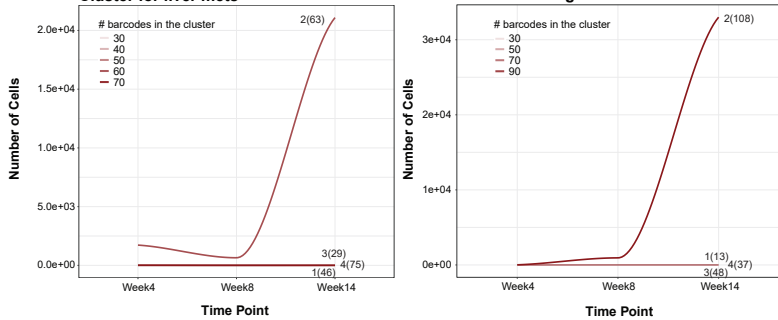


\* Red: Number of primary tumor that %>0 at all time points  
 \* Green: Mets to liver  
 \* Yellow: Mets to lung

**C**

Cluster for liver mets

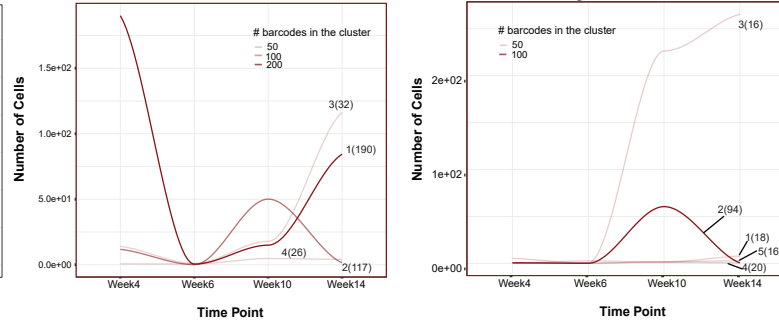
Cluster for lung mets



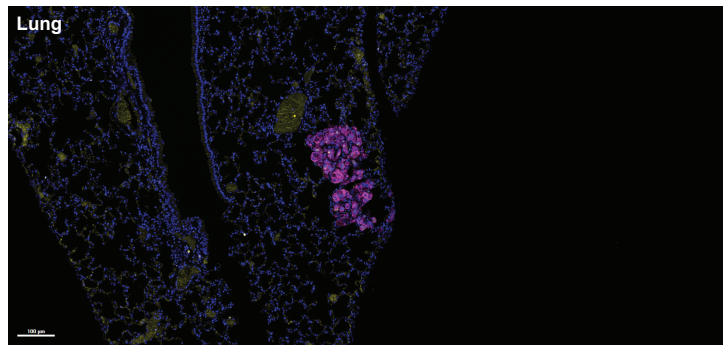
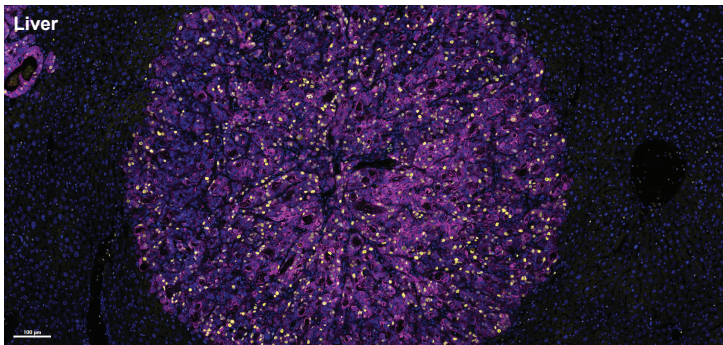
**D**

Cluster for liver mets

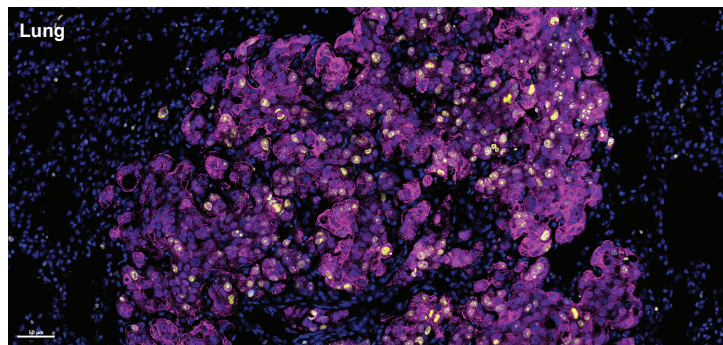
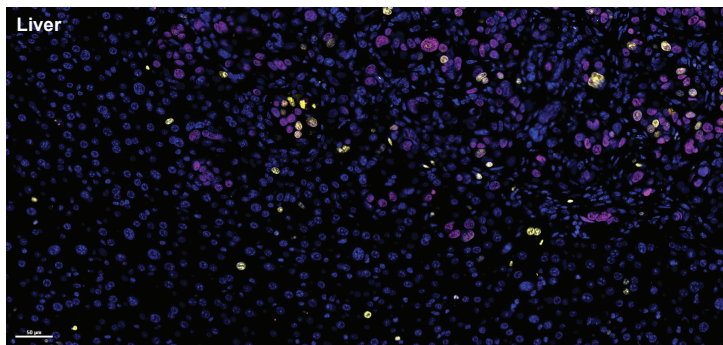
Cluster for lung mets



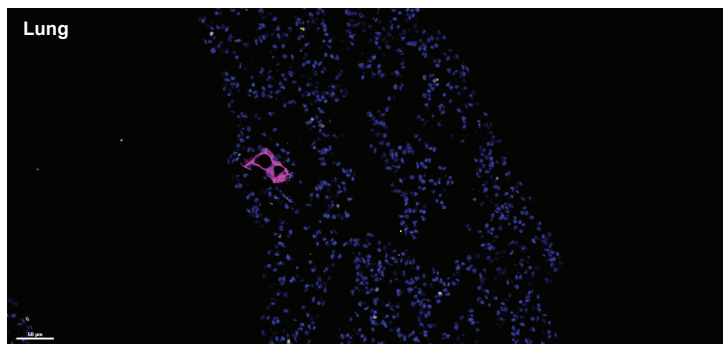
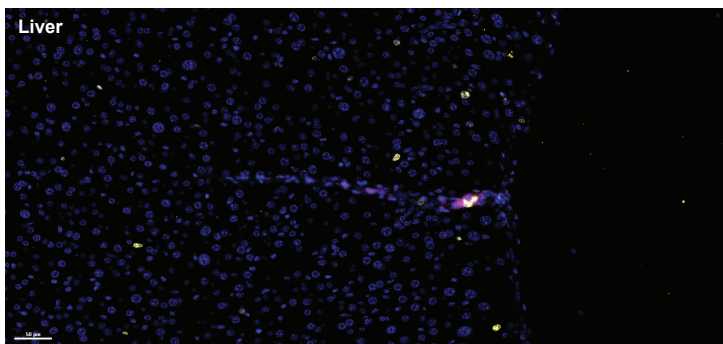
**E**



**F**



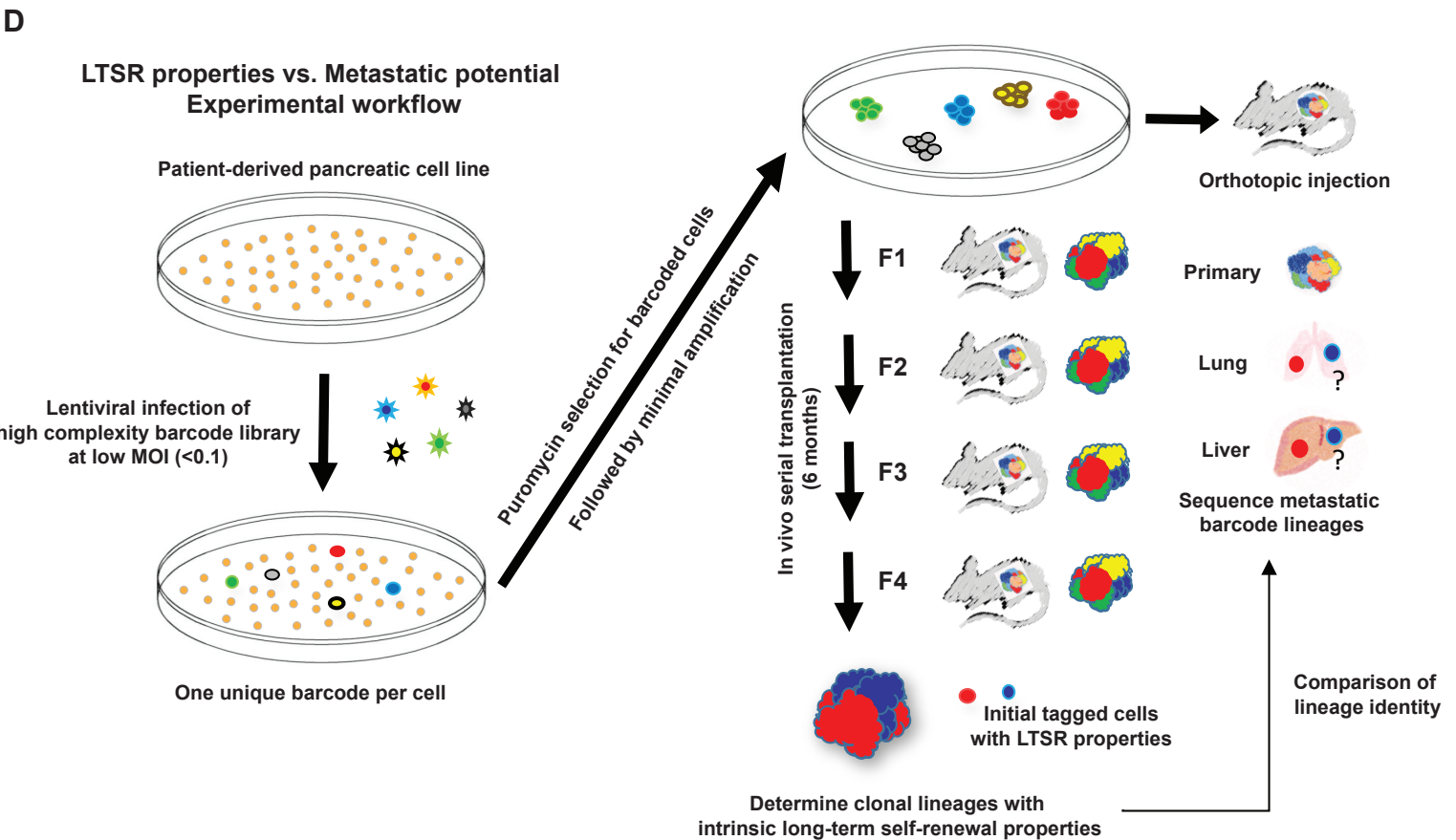
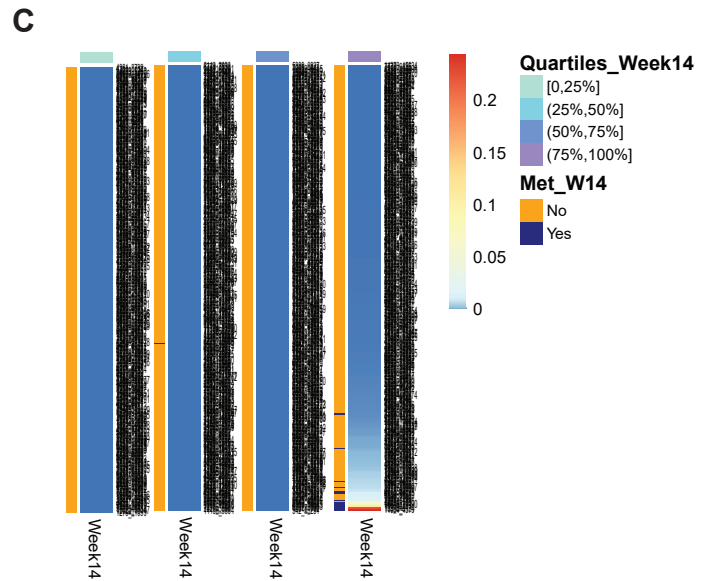
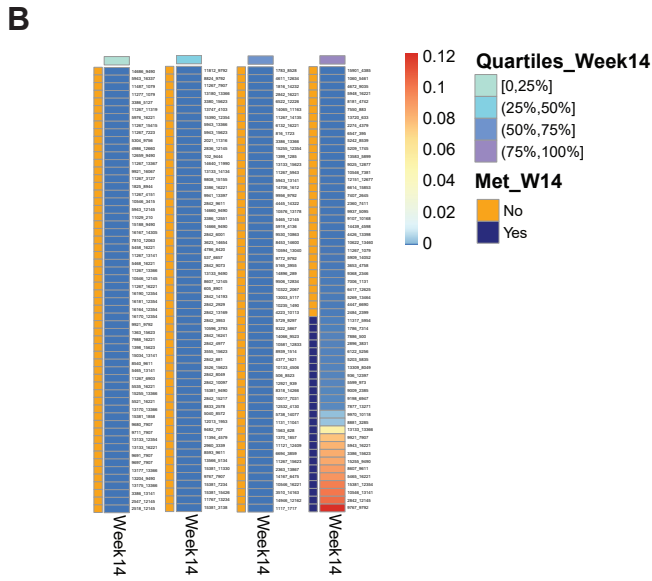
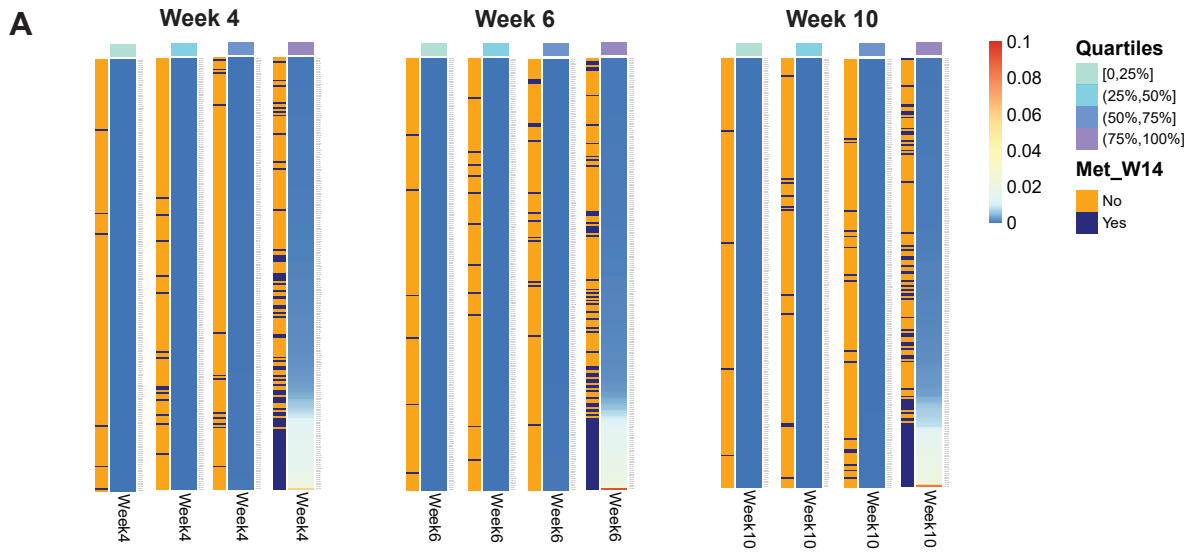
**G**



### Supplementary Figure 3. PDX-derived models exhibit distinct organotropisms

**a,b**, Venn diagram of the number of clones detected in the primary tumor, liver, and lungs of PATC69 (**a**) and PATC108 (**b**) at least at one time point. **c,d**, Dynamic subclonal growth of PATC69 (**c**) and PATC108 (**d**) in liver and lung. Cell number at each time point is converted based on spike-in scales. Lineage behavior was grouped into discrete dynamic growth patterns (clusters) over time. The numbers outside the brackets indicate the cluster name, and the number within the brackets indicate the exact number of barcodes within the cluster (darker colors are associated with larger number of barcodes within the cluster). **e-g**, Liver and lungs from PATC124 (**e**), PATC69 (**f**) and PATC108 (**g**) mice at 14 weeks were harvested and stained with anti-HLA (magenta) and anti-Ki67 (yellow). Cell nuclei were stained with DAPI (blue). Scale bar=100  $\mu\text{m}$  for PATC124; scale bar=50  $\mu\text{m}$  for PATC69 and PATC108.

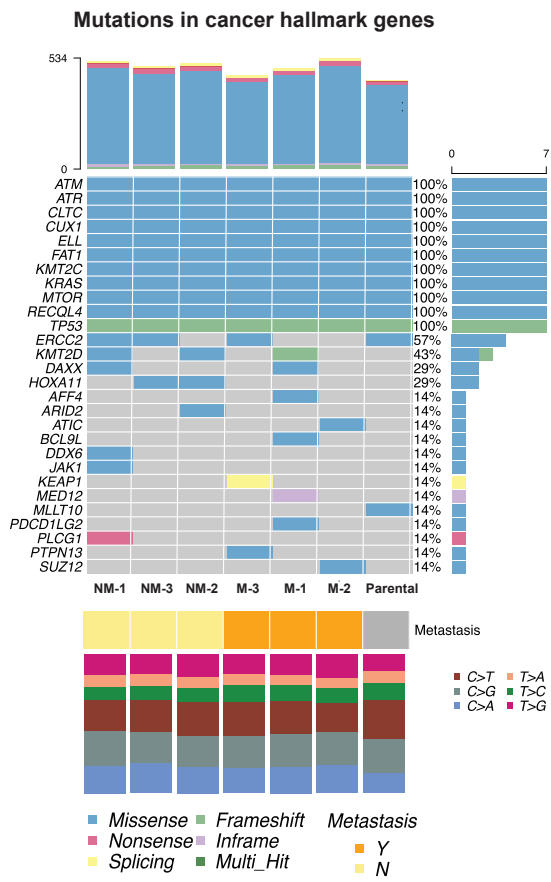
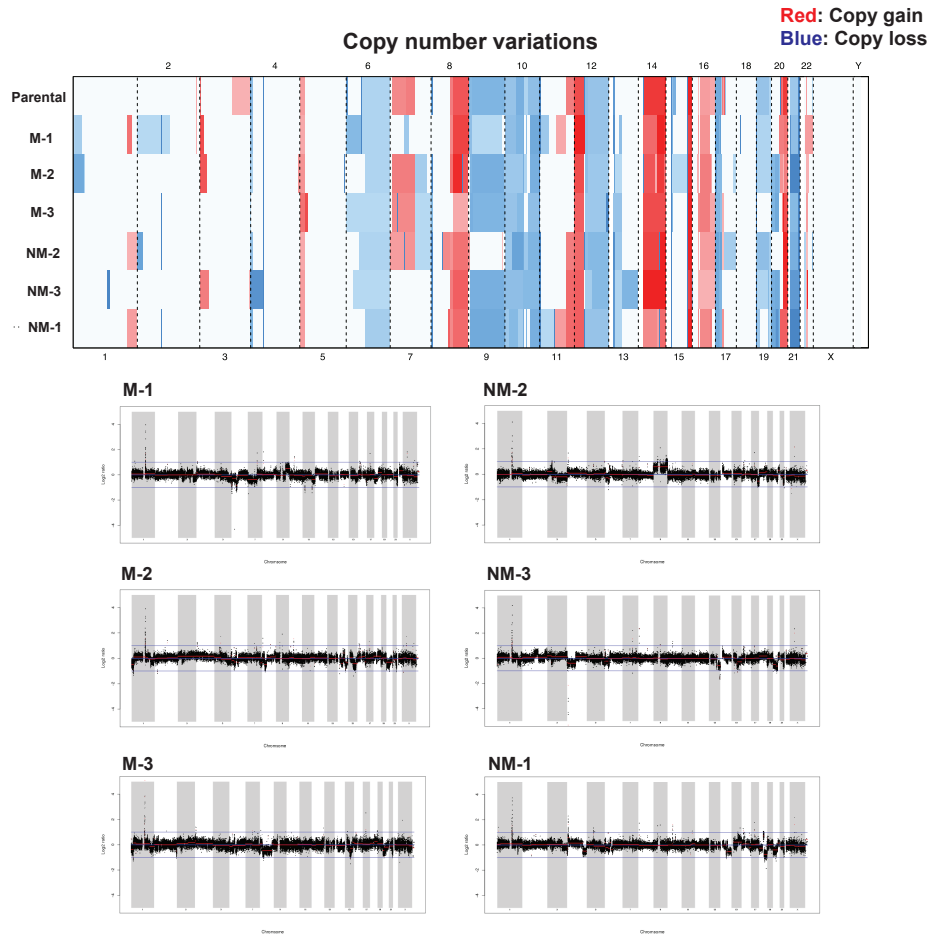
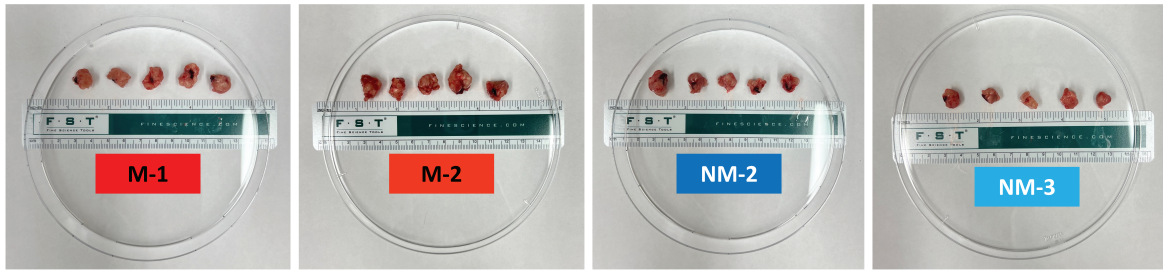
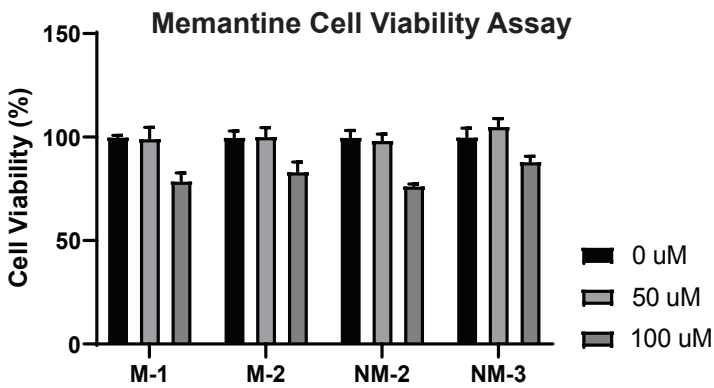
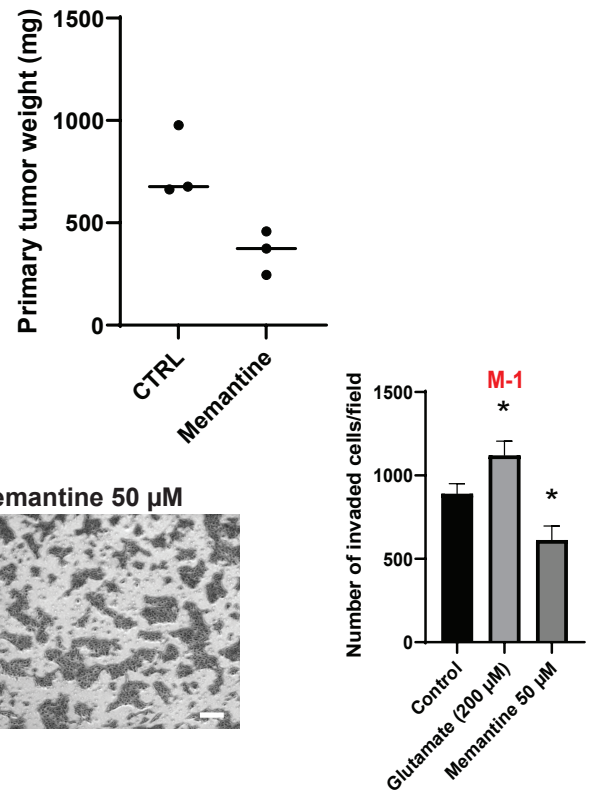
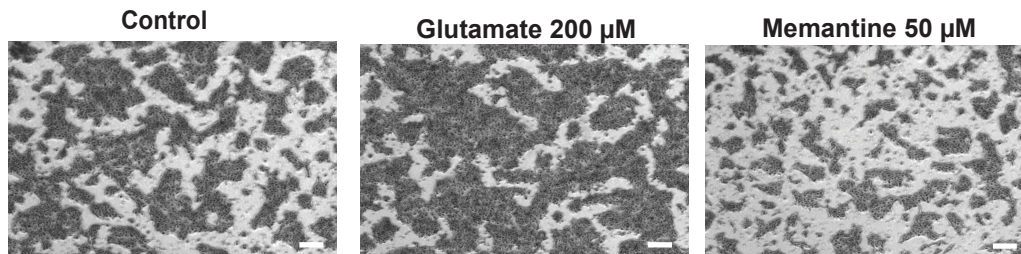
**Fig. S4**





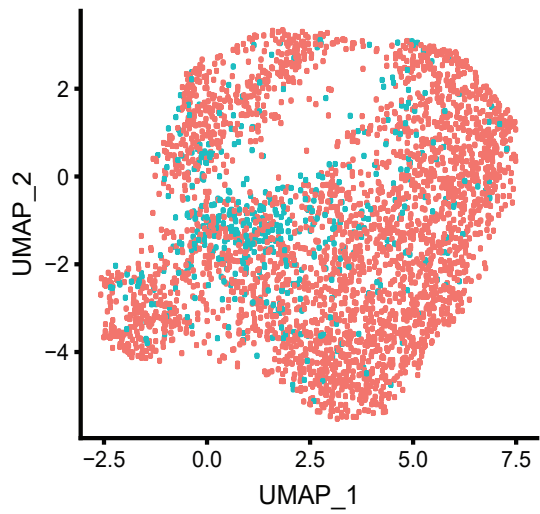
#### **Supplementary Figure 4. Clonal abundance is highly correlated with metastatic potential**

**a**, Heatmap of subclonal abundance (percentage) in the PATC124 primary tumor at weeks 4, 6 and 10 with metastasis status (yes >200 tumor cells / no <200 tumor cells) at week 14. Quartiles are as defined in Fig. 2. Metastasis of each subclone is indicated on the left of each heat map in quartiles (yellow, no dissemination; blue, dissemination). **b,c**, Heatmap of average subclonal abundance (percentage) in the PATC69 (**b**) and PATC108 (**c**) primary tumors with metastasis status (yes >200 tumor cells / no <200 tumor cells ) at week 14. Barcodes were divided into quartiles (0%–25%, 25%–50%, 50%–75%, and 75%–100%) on the basis of their percent of total tumor mass. Metastasis of each subclone is indicated on the left of each heat map in quartiles (yellow, no dissemination; blue, dissemination). **d**, Experimental workflow of parallel metastatic potential and LTSR studies. PATC124 cells were barcoded with a high-complexity barcode library at low MOI and selected with puromycin. The barcoded cells were minimally amplified to achieve uniformity across barcoded clones as well as cell number. After taking an aliquot for baseline barcode analysis, the barcoded cells were split in half for the two studies. For the metastatic potential study, n = 3 animals received orthotopic injection in the pancreas, and animals were euthanized after 3 months to collect primary tumor, liver, and lungs for NGS barcode analysis. For the LTSR study, n = 3 animals were injected in the F1 generation followed by serial transplantation into recipient animals every 1.5 months through F4 animals (total duration of study was 6 months). Primary tumors were collected for NGS barcode analysis from all animals in generations F1-F4.

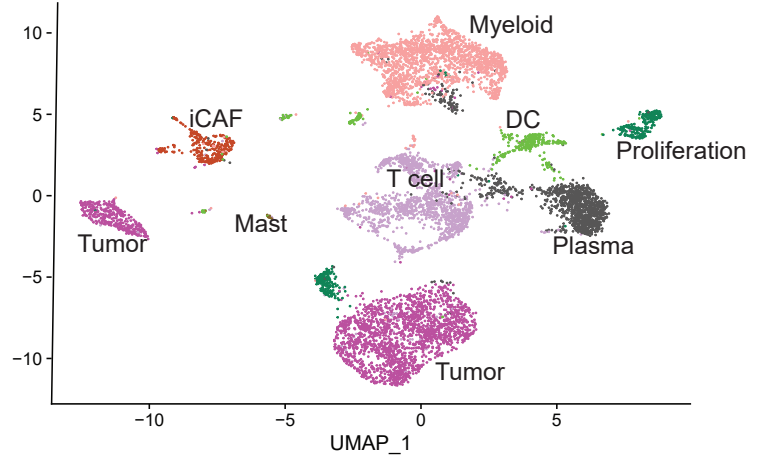
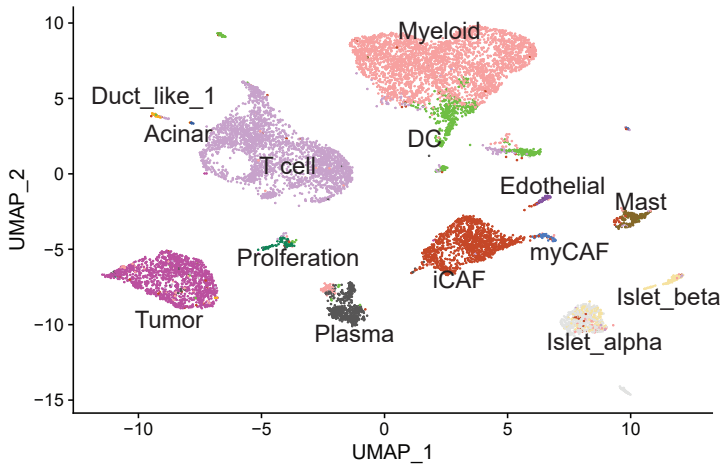
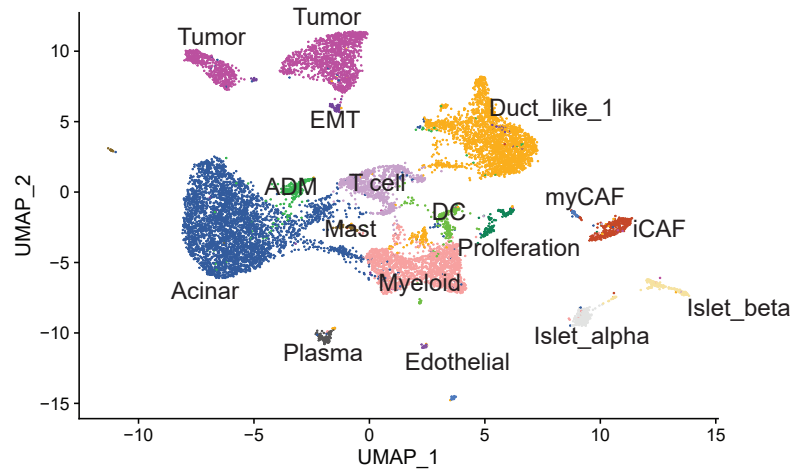
**Fig. S5****A****B****C****D****F****E**

### **Supplementary Figure 5. Genomic and functional characterization of isolated clones**

**a**, 6 PATC124 isogenic clones with differential metastasis potential and their parental population were submitted for WES to identify mutations in hallmark cancer genes. **b**, CNV profiling results from the 6 PATC124 isogenic clones and parental cells compared to a normal diploid genome. Data are shown in aberration plot (top, copy number gain in red and copy number loss in blue) and CNV plot (bottom; Log<sub>2</sub> ratio; red lines indicate copy segments). **c**, Monoclonal primary tumor images of 2 metastatic (M-1 and M-2) and two non-metastatic (NM-2 and NM-3) PATC124 clones. **d**, MTT assay to evaluate effects of a range of memantine concentrations on viability of PATC124 clones. Data are presented as mean  $\pm$  SD of two independent experiments. **e**, Representative images of invasion assay of PATC124 M-1 metastatic clone grown with glutamate (NMDAR agonist) or memantine (NMDAR antagonist). Quantification of invaded cells per field is shown as mean  $\pm$  SD of two independent experiments. Statistical significance was assessed using one-way ANOVA. Scale bar = 200  $\mu$ m. **f**, PATC124 bi-clonal (M-1 and M-2) primary tumor weight of untreated control and memantine treated group as in figure 5h.

**A****Single cell RNA-seq (n = 3397)**

■ All others (n=2944)  
■ Met (n=453)

**B****HT264P****C****HT270P****D****HT288P**

**Supplementary Figure 6. scRNA-seq of different human pancreatic cancer cells**

**a**, The 100 most enriched and 100 most downregulated genes from transcriptomic analysis as in figure 5a were used to derive a pro-met signature. ScRNA-seq analysis of PATC124 cells (n = 3,397) was used to identify clones with metastatic potential. **b-d**, Overview of all cell types profiled in the scRNA-seq cohorts as in Figure 6a-c.